PAPER • OPEN ACCESS

Cartesian product of synchronization transitions and hysteresis

New Journal of Physics
The open access journal at the forefront of physics

Deutsche Physikalische Gesellschaft DPG
IOP Institute of Physics

Published in partnership with: Deutsche Physikalische Gesellschaft and the Institute of Physics

OPEN ACCESS

RECEIVED
7 September 2017

REVISED
25 October 2017

ACCEPTED FOR PUBLICATION
10 November 2017

PUBLISHED
14 December 2017

PAPER

Cartesian product of synchronization transitions and hysteresis

Changsu Wang[1], **Yong Zou**[1,2], **Shuguang Guan**[1] **and Jürgen Kurths**[2,3]

[1] Department of Physics, East China Normal University, Shanghai, People's Republic of China
[2] Potsdam Institute for Climate Impact Research, Potsdam, Germany
[3] Saratov State University, Saratov, Russia

E-mail: yzou@phy.ecnu.edu.cn

Keywords: synchronization transition, hysteresis, Kuramoto model, Cartesian product graphs

Abstract

We present theoretical results when applying the Cartesian product of two Kuramoto models on different network topologies. By a detailed mathematical analysis, we prove that the dynamics on the Cartesian product graph can be described by the canonical equations as the Kuramoto model. We show that the order parameter of the Cartesian product is the product of the order parameters of the factors. On the product graph, we observe either continuous or discontinuous synchronization transitions. In addition, under certain conditions, the transition from an initially incoherent state to a coherent one is discontinuous, while the transition from a coherent state to an incoherent one is continuous, presenting a mixture state of first and second order synchronization transitions. Our numerical results are in a good agreement with the theoretical predictions. These results provide new insight for network design and synchronization control.

1. Introduction

Synchronization in nonlinear sciences is an emergent property that occurs in a broad range of dynamical systems, including neural signaling, the beating of the heart, fire-fly light waves, or power grids [1]. Kuramoto phase model is a paradigmatic example in synchronization analysis [2, 3]. This model consists of self-sustained phase oscillators rotating at heterogeneous intrinsic frequencies coupled through the sine of their phase differences [4, 5]. A transition from an initially incoherent state to a fully coherent state takes place when the coupling strength exceeds a critical threshold, which explains many collective behaviors in nature, science, society and technology [1, 3]. There have been rapid developments in the study of the Kuramoto model focusing on the effects of network structures on synchronization, e.g., from the traditional all-to-all coupling to heterogeneous complex network topologies [6, 7]. In the case of complex network structures, several models have been proposed to study effects of small-world structures, communities, degree correlations and multi-layer network structures [8]. Recent findings of the Kuramoto model on different network topologies have been reviewed in [9].

It is important to emphasize that most likely continuous synchronization transitions can be observed in these Kuramoto models on top of networks. Namely, the order parameter which characterizes the degree of synchronization grows continuously when the coupling strength passes the critical threshold. In other words, when the coupling strength is increased progressively, the sizes of the synchronized clusters grow gradually [10]. The findings of discontinuous phase transition to synchronization (also known as abrupt explosive synchronization) have triggered several rapid investigations [11–14], which is a consequence of correlations between network structure and local dynamics. The most intriguing phenomenon is that hysteresis has been largely observed in explosive synchronization [11]. More specifically, the network shows an explosive jump from an incoherent state to a coherent one when the coupling strength is increased adiabatically, which is conveniently called forward continuation curve below. In addition, it shows a sudden drop from the coherent state to the incoherent state when the coupling strength is decreased progressively (backward continuation curve). There is a clear hysteresis area because these two curves (forward and backward) do not overlap. In the case of continuous synchronization transitions, the forward and backward curves are overlapped. Hysteresis is a

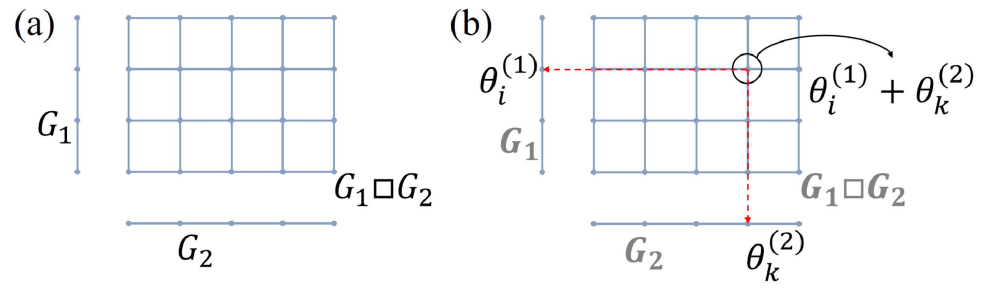

Figure 1. Panel (a): Cartesian product of two factors (chains) G_1 and G_2. Panel (b) product of two phase oscillators using the Kronecker sum.

fundamental property of a first order phase transition, which shares some analogies with explosive percolation [15]. The hysteresis behavior at the onset of synchronization has been widely observed in various situations, such as scale-free networks [11, 16], electronic circuits [12, 17], time delayed systems [18], and a second order Kuramoto model [19]. Recent studies also focused on the importance of the frequency distribution [20], noise effects [21], various generalizations of the coupling patterns [22, 23], and multi-layer networks [14].

Usually, the continuous and discontinuous synchronization transitions are separately discussed in the literature [15], because of the different requirements of network configurations and local dynamics. Here, we propose an algorithm based on graph product operation, which allows for discussing continuous and discontinuous synchronization transitions in a unified framework. In particular, we construct the Kuramoto model by the Cartesian product, which is one of the basic operations on a graph [24]. This graph operation helps to find hysteretic synchronization transitions with more intriguing phenomena. In particular, we find that the forward transition curve is discontinuous while the backward transition is continuous. Note that the effects of graph operations on the synchronization behavior remained largely unclear, although some discussions on the synchronizabilities have been presented in terms eigenspectra [25, 26]. To the best of our knowledge, our work is the first attempt to address the effects of the Cartesian product on the synchronization behavior of the Kuramoto model, resulting in a mixture state of both continuous and discontinuous transitions.

Let us start by considering the Kuramoto model on a complex network. We consider n phase oscillators on top of a complex network G in the following framework without loss of generality

$$\frac{\mathrm{d}\theta_i}{\mathrm{d}t} = \omega_i + \lambda \sum_{j=1}^{n} A_{ij} \sin(\theta_j - \theta_i), \quad (i = 1, 2, \cdots, n), \tag{1}$$

where ω_i are the natural frequencies taken from a certain distribution, λ is the coupling strength, and A_{ij} is the adjacency matrix of the network. Oscillator i is coupled with j if there is a link between node i and j, namely, $A_{ij} = 1$. Otherwise, $A_{ij} = 0$ means that i and j are not connected. The Kuramoto order parameter R is defined as

$$R = \left| \frac{1}{n} \sum_{j=1}^{n} \mathrm{e}^{\mathrm{i}\theta_j} \right|_t, \tag{2}$$

where the notation $|\cdot|_t$ denotes the time average of the absolute value over $t \gg 1$. Small values of R indicate incoherent behavior. In contrast, as $R \to 1$ we encounter a highly coherent state.

2. Product of Kuramoto models

We start by introducing the method of Cartesian product of graphs, which is an important way to construct a bigger graph and plays an important role in network design and analysis.

Given two nonempty graphs $G_1 = (V_1, E_1)$ and $G_2 = (V_2, E_2)$, the Cartesian product $G_1 \square G_2$ of the two graphs is a graph such that: (i) the vertex set of $G_1 \square G_2$ is the Cartesian product $V_1 \times V_2$. For example, given vertices i of G_1 and k of G_2, we denote the vertex of $G_1 \square G_2$ as $\langle ik \rangle$; (ii) two vertices $\langle ik \rangle$ and $\langle jl \rangle$ are connected in $G_1 \square G_2$ if and only if (a) $i = j$ and k is adjacent with l in G_2, or (b) $k = l$ and i is adjacent with j in G_1. The graphs G_1 and G_2 are called factors of the product $G_1 \square G_2$ [24]. In figure 1(a), we give an example of the Cartesian product of two chains and the resulting graph is a regular lattice. Further examples of the Cartesian product graphs are illustrated by two factor subgraphs of stars (Figure 2(a)), two rings (Figure 2(e)), and one star and one ring (figure 2(i)).

The Cartesian product of graphs is a commutative, associative binary operation on graphs [27]. It has many useful properties, most of which can be derived from the factors. In particular, the adjacency matrix of $G_1 \square G_2$ is

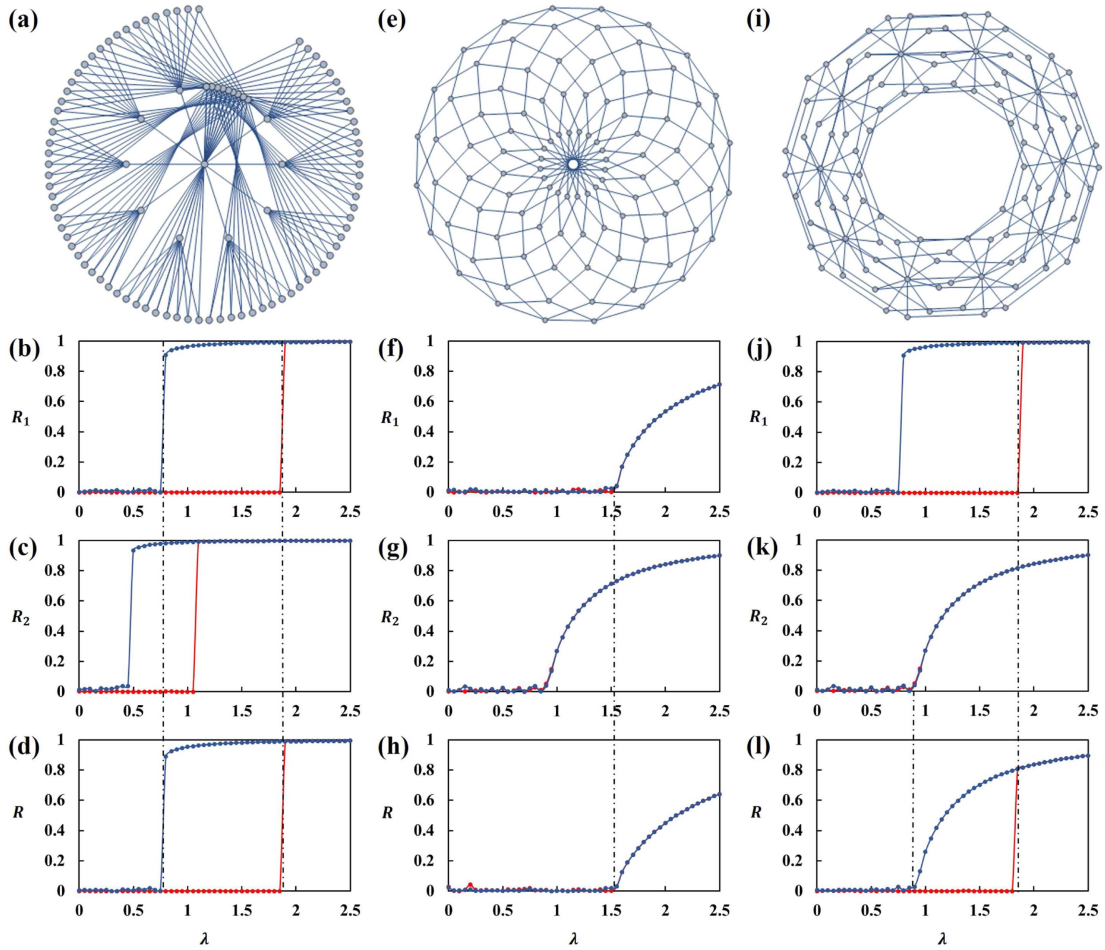

Figure 2. Numerical results for synthetic synchronization transitions. Panels (a)–(d): discontinuous transitions, (e)–(h) continuous transitions, and (i)–(l) mixture of continuous transition for the backward direction and discontinuous transition for the forward direction. Equal sizes for factor graphs G_1 and G_2 are used ($n_1 = n_2 = 10$). Cartesian product graph $G_1\square G_2$ of (a): two stars; (e) two rings; and (i) G_1 is a star and G_2 is a ring. Panels (b), (f) and (j) are order parameters for synchronization transition curves on the factor G_1, where the red curve is the forward curve and the blue is the backward curve. The similar curves for factor G_2 are shown in panels (c), (g) and (k). Panels (d), (h) and (l) are order parameters for synchronization transition curves on the product $G_1\square G_2$ graph. Vertical dashed lines are theoretical predictions as summarized in table 3.

the Kronecker sum of the adjacency matrices of G_1 and G_2, namely, $\boldsymbol{A}(G_1\square G_2) = \boldsymbol{A}(G_1) \oplus \boldsymbol{A}(G_2)$ (see appendix A for details on the Kronecker product and sum of matrices).

Theorem. *Given two independent Kuramoto models on factor graphs G_1 and G_2 (n_1 oscillators on G_1 and n_2 oscillators on G_2, respectively), the definition of the phase of the node $\langle ik\rangle$ as $\theta_{\langle ik\rangle} = \theta_i^{(1)} + \theta_k^{(2)}$ yields the canonical equations of the Kuramoto model on the Cartesian product graph $G_1\square G_2$. The natural frequency of oscillator $\langle ik\rangle$ is $\omega_{\langle ik\rangle} = \omega_i^{(1)} + \omega_k^{(2)}$ and the $n_1 n_2$ oscillators are coupled through the sine functions of their phase differences.*

Proof. An example of constructing Cartesian product from two chain models is shown in figure 1(b). For two independent graphs G_1 and G_2, the adjacency matrices are $\boldsymbol{A}^{(1)}$ and $\boldsymbol{A}^{(2)}$ respectively. The Kuramoto models on the respective factors are written as

$$G_1: \frac{\mathrm{d}\theta_i^{(1)}}{\mathrm{d}t} = \omega_i^{(1)} + \lambda \sum_{j=1}^{n_1} A_{ij}^{(1)} \sin(\theta_j^{(1)} - \theta_i^{(1)}), \quad (i = 1, 2, \cdots, n_1), \tag{3}$$

$$G_2: \frac{\mathrm{d}\theta_k^{(2)}}{\mathrm{d}t} = \omega_k^{(2)} + \lambda \sum_{l=1}^{n_2} A_{kl}^{(2)} \sin(\theta_l^{(2)} - \theta_k^{(2)}), \quad (k = 1, 2, \cdots, n_2). \tag{4}$$

We define $\theta_{\langle ik\rangle} = \theta_i^{(1)} + \theta_k^{(2)}$, then the time derivatives of the phases $\theta_{\langle ik\rangle}$ on the Cartesian product $G_1\square G_2$ are

$$\frac{\mathrm{d}\theta_{\langle ik\rangle}}{\mathrm{d}t} = \frac{\mathrm{d}\theta_i^{(1)}}{\mathrm{d}t} + \frac{\mathrm{d}\theta_k^{(2)}}{\mathrm{d}t} \tag{5}$$

$$= \omega_i^{(1)} + \lambda\sum_{j=1}^{n_1} A_{ij}^{(1)}\sin(\theta_j^{(1)} - \theta_i^{(1)}) + \omega_k^{(2)} + \lambda\sum_{l=1}^{n_2} A_{kl}^{(2)}\sin(\theta_l^{(2)} - \theta_k^{(2)})$$

$$= \omega_i^{(1)} + \omega_k^{(2)} + \lambda\sum_{j=1}^{n_1}\sum_{l=1}^{n_2} A_{ij}^{(1)}\delta_{kl}\sin(\theta_j^{(1)} - \theta_i^{(1)} + \theta_l^{(2)} - \theta_k^{(2)}) \tag{6}$$

$$+\lambda\sum_{j=1}^{n_1}\sum_{l=1}^{n_2}\delta_{ij}A_{kl}^{(2)}\sin(\theta_j^{(1)} - \theta_i^{(1)} + \theta_l^{(2)} - \theta_k^{(2)}) \tag{7}$$

$$= \omega_i^{(1)} + \omega_k^{(2)} + \lambda\sum_{\langle jl\rangle} A_{ij}^{(1)}\delta_{kl}\sin(\theta_{\langle jl\rangle} - \theta_{\langle ik\rangle}) + \lambda\sum_{\langle jl\rangle}\delta_{ij}A_{kl}^{(2)}\sin(\theta_{\langle jl\rangle} - \theta_{\langle ik\rangle}) \tag{8}$$

$$= \omega_i^{(1)} + \omega_k^{(2)} + \lambda\sum_{\langle jl\rangle}(A_{ij}^{(1)}\delta_{kl} + \delta_{ij}A_{kl}^{(2)})\sin(\theta_{\langle jl\rangle} - \theta_{\langle ik\rangle}). \tag{9}$$

The result of equation (9) has exactly the same expression as the equation of the Kuramoto model. Furthermore, it is easy to recognize that the natural frequencies are $\omega_{\langle ik\rangle} = \omega_i^{(1)} + \omega_k^{(2)}$. ♯

Remark 1. There are no interactions between the two factors G_1 and G_2 and the dynamics of oscillators on G_1 evolves independently with oscillators on G_2. The oscillator dynamics on the Cartesian product graph $G_1\square G_2$ is reconstructed by means of the summation of the respective phases on G_1 and G_2. The advantage of defining the phase of the node on the product graph as the summation of the respective phases of the factor subgraphs yields the canonical equations of the Kuramoto model on $G_1\square G_2$. In addition, the Cartesian product operation can be easily generalized to the case of n subgraphs because $G_1\square G_2$ and $G_2\square G_1$ are isomorphic (the operation is commutative). Furthermore this operation is associative. For instance, given three factor subgraphs G_1, G_2 and G_3, the phase summation of three factors results in the traditional equations as the Kuramoto model on the product graph as $(G_1\square G_2)\square G_3$ and $G_1\square(G_2\square G_3)$ are isomorphic. With the commutative and associative properties of the phase summation, we generalize the theorem to the case of n factor subgraphs straightforwardly.

Lemma. *The order parameter R on the Cartesian product graph of $G_1\square G_2$ is the product of the order parameters R_1 and R_2 of two independent factors, namely, $R = R_1R_2$.*

Proof. The order parameter R on the Cartesian product graph is computed as follows:

$$R = \left|\frac{1}{n_1n_2}\sum_{\langle jl\rangle}\mathrm{e}^{\mathrm{i}\theta_{\langle jl\rangle}}\right| \tag{10}$$

$$= \left|\frac{1}{n_1n_2}\sum_{j=1}^{n_1}\sum_{l=1}^{n_2}\mathrm{e}^{\mathrm{i}(\theta_j^{(1)}+\theta_l^{(2)})}\right| \tag{11}$$

$$= \left|\frac{1}{n_1}\sum_{j=1}^{n_1}\mathrm{e}^{\mathrm{i}\theta_j^{(1)}}\right|\left|\frac{1}{n_2}\sum_{l=1}^{n_2}\mathrm{e}^{\mathrm{i}\theta_l^{(2)}}\right| \tag{12}$$

$$= R_1R_2.\sharp. \tag{13}$$

Therefore, we prove that the order parameter R is fully determined by the two factors R_1 and R_2. Furthermore, R does not converge if any of the order parameters of the two factors (either R_1 or R_2) does not converge.

In addition, for n factor subgraphs, it is straightforward to show that the order parameter R on the product graph is the order parameters of n factors. For instance, given three factors G_1, G_2 and G_3, the order parameter R of the product $G_1\square G_2\square G_3$ is $R = R_1R_2R_3$.

3. Kuramoto model on star and ring structures

Before showing the main results of this work, we discuss the synchronization transitions when implementing the Kuramoto models on single star and ring structures (see appendix E for further results on chain structures and appendix F for trees). Both stars, rings, chains and trees of oscillators have been studied extensively in

synchronization analysis because they are considered to be motifs to build complex networks [28–35]. Here, we show the critical coupling threshold values for synchronization on these topologies.

First, taking into account different network topologies, we rewrite the Kuramoto model (equation (1)) in terms of link representation in the following. Assume that there are n nodes and m links in a network which is represented by the adjacency matrix $\boldsymbol{A} \in \mathbb{R}^{n\times n}$. In general, the link incidence matrix $\boldsymbol{B} \in \mathbb{R}^{m\times n}$ of a directed network is defined as

$$B_{\alpha i} = \begin{cases} +1 & i \text{ is the starting node of link } \alpha, \\ 0 & \text{otherwise}, \\ -1 & i \text{ is the end node of link } \alpha, \end{cases} \tag{14}$$

where α is the link and i is the oscillator. Note that no difference appears when using the above matrix $\boldsymbol{B}$ to represent an undirected network. Therefore, the Kuramoto model (equation (1)) is rewritten in the following compact matrix form

$$\frac{\mathrm{d}\boldsymbol{\theta}}{\mathrm{d}t} = \boldsymbol{\omega} - \lambda \boldsymbol{B}^T \sin \boldsymbol{B}\boldsymbol{\theta}, \tag{15}$$

where $\boldsymbol{\theta} = (\theta_1, \theta_2, \ldots, \theta_n)^T$, $\boldsymbol{\omega} = (\omega_1, \omega_2, \ldots, \omega_n)^T$, and T is the transpose operation to the corresponding vectors. Furthermore, the sine function acts on the phase vector one by one, e.g., we define $\sin(\theta_1, \theta_2, \theta_3)^T \triangleq (\sin\theta_1, \sin\theta_2, \sin\theta_3)^T$.

It is straightforward to show that the compact form representation of the Kuramoto model (equation (15)) is identical to the canonical equations (equation (1)) (in appendix B, we show the equivalence for the two expressions). We then compute the average phase of all oscillators as $\bar{\theta} = \frac{1}{n}\sum_{i=1}^{n}\theta_i$, which further suggests that the population rotates at the same average frequency $\bar{\omega}$ as follows

$$\frac{\mathrm{d}\bar{\theta}}{\mathrm{d}t} = \frac{1}{n}\sum_{i=1}^{n}\frac{\mathrm{d}\theta_i}{\mathrm{d}t} = \frac{1}{n}\sum_{i=1}^{n}\omega_i + \frac{\lambda}{n}\sum_{i=1}^{n}\sum_{j=1}^{n}\sin(\theta_j - \theta_i) = \bar{\omega}. \tag{16}$$

Synchronization is achieved when the phase difference between all oscillators is a constant. Therefore, the synchronization condition is equivalently represented by

$$\frac{\mathrm{d}(\boldsymbol{\theta} - \bar{\boldsymbol{\theta}})}{\mathrm{d}t} = \boldsymbol{\omega} - \bar{\boldsymbol{\omega}} - \lambda \boldsymbol{B}^T \sin \boldsymbol{B}\boldsymbol{\theta} = \boldsymbol{0}, \tag{17}$$

where $\bar{\boldsymbol{\theta}} = (\bar{\theta}, \bar{\theta}, \cdots, \bar{\theta})^T$, $\bar{\boldsymbol{\omega}} = (\bar{\omega}, \bar{\omega}, \cdots, \bar{\omega})^T$ representing each oscillator has the same frequency as the population averaged frequency. Thus, synchronization suggests that there is a solution $\boldsymbol{\theta}$ in the following equation:

$$\lambda \boldsymbol{B}^T \sin \boldsymbol{B}\boldsymbol{\theta} = \boldsymbol{\omega} - \bar{\boldsymbol{\omega}}. \tag{18}$$

In appendix D, we provide detailed discussions on the existence and uniqueness of the solutions to the linear equation (18). In addition, we prove that a solution always exists for connected networks. We summarize the results for two typical networks in terms of the following corollaries:

Corollary 1. *For n oscillators coupled in a star topology, the necessary condition of synchronization is $\lambda \geqslant \lambda_c = \max_{2\leqslant i\leqslant n}|\omega_i - \bar{\omega}|$, where $\bar{\omega}$ is the average frequency and the maximum function runs over all leaf nodes i.*

Proof. The hub node in the network has index 1 and leaf nodes are $2, 3, \ldots, n$. The incidence matrix is

$$\boldsymbol{B} = \begin{pmatrix} 1 & -1 & 0 & \ldots & 0 \\ 1 & 0 & -1 & \ldots & 0 \\ \vdots & \vdots & \vdots & \ddots & \vdots \\ 1 & 0 & 0 & \ldots & -1 \end{pmatrix} \tag{19}$$

and the Moore–Penrose pseudo-inverse (see appendix C for definitions) reads

$$\boldsymbol{B}^{+T} = \begin{pmatrix} \frac{1}{n} & -\frac{n-1}{n} & \frac{1}{n} & \ldots & \frac{1}{n} \\ \frac{1}{n} & \frac{1}{n} & -\frac{n-1}{n} & \ldots & \frac{1}{n} \\ \vdots & \vdots & \vdots & \ddots & \vdots \\ \frac{1}{n} & \frac{1}{n} & \frac{1}{n} & \ldots & -\frac{n-1}{n} \end{pmatrix}. \tag{20}$$

In addition, we have

$$\boldsymbol{B}^{+T}\boldsymbol{\omega} = \begin{pmatrix} \bar{\omega} - \omega_2 \\ \bar{\omega} - \omega_3 \\ \vdots \\ \bar{\omega} - \omega_n \end{pmatrix}. \tag{21}$$

A necessary condition for synchronization is

$$\lambda \geqslant \lambda_c = \|\boldsymbol{B}^{+T}\boldsymbol{\omega}\|_\infty = \max_\alpha|[\boldsymbol{B}^{+T}\boldsymbol{\omega}]_\alpha| = \max_{2\leqslant i\leqslant n}|\omega_i - \bar{\omega}|, \tag{22}$$

where the maximum function runs over all leaf nodes i. ♯

Remark 2. If all leaf nodes have the same frequency $\omega_2 = \omega_3 = \cdots = \omega_n = \omega$ and the hub node has $\omega_1 = (n-1)\omega$, we obtain the synchronization threshold $\lambda_c = \frac{n-2}{n}\omega$ which is the same as reported in [13, 36].

Remark 3. The Kuramoto model on either a star or a chain can be generalized to a more general framework of a tree structure. The necessary condition to synchronization of the Kuramoto model on a tree is $\lambda_c \geqslant \max_{1\leqslant\alpha\leqslant m}|\sum_{i\in A_\alpha}(\omega_i - \bar{\omega})|$, where the maximum function runs over all links that are included in the connected component A_α if link α is removed. The details are provided in appendix F.

Corollary 2. *For n oscillators coupled in a ring, if n is an even number and $\omega_i = -\omega_{i+n/2}$, a necessary condition for synchronization is $\lambda \geqslant \lambda_c = \|\boldsymbol{B}^{+T}\boldsymbol{\omega}\|_\infty = \max|[\boldsymbol{B}^{+T}\boldsymbol{\omega}]_\alpha|$, where the maximum function runs over all links α.*

Proof. The incidence matrix is

$$\boldsymbol{B} = \begin{pmatrix} -1 & 0 & 0 & \dots & 1 \\ 1 & -1 & 0 & \dots & 0 \\ 0 & 1 & -1 & \dots & 0 \\ \vdots & \vdots & \vdots & \ddots & \vdots \\ 0 & 0 & 0 & -1 & 0 \\ 0 & 0 & 0 & 1 & -1 \end{pmatrix} \tag{23}$$

and the Moore–Penrose pseudo-inverse reads

$$\boldsymbol{B}^{+T} = \begin{pmatrix} -\frac{n-1}{2n} & -\frac{n-3}{2n} & -\frac{n-5}{2n} & \cdots & \frac{n-3}{2n} & \frac{n-1}{2n} \\ \frac{n-1}{2n} & -\frac{n-1}{2n} & -\frac{n-3}{2n} & \cdots & \frac{n-5}{2n} & \frac{n-3}{2n} \\ \vdots & \vdots & \vdots & \ddots & \vdots & \vdots \\ -\frac{n-3}{2n} & -\frac{n-5}{2n} & -\frac{n-7}{2n} & \cdots & \frac{n-1}{2n} & -\frac{n-1}{2n} \end{pmatrix}. \tag{24}$$

For the notation convenience below, we denote the first row of $\boldsymbol{B}^{+T}$ as $\boldsymbol{b} = \left(-\frac{n-1}{2n}, -\frac{n-3}{2n}, \cdots, \frac{n-1}{2n}\right)$. Then, the second row of $\boldsymbol{B}^{+T}$ has a recursive relationship by putting the last entry to the beginning of $\boldsymbol{b}$. Introducing a permutation matrix $\boldsymbol{P}$ that shifts the last entry to the beginning, the second row is denoted as $\boldsymbol{b}\boldsymbol{P}^T$. With this notation, we re-write the Moore–Penrose pseudo-inverse as

$$\boldsymbol{B}^{+T} = (\boldsymbol{b}^T, \boldsymbol{P}\boldsymbol{b}^T, \boldsymbol{P}^2\boldsymbol{b}^T, \cdots, \boldsymbol{P}^{n-1}\boldsymbol{b}^T)^T. \tag{25}$$

In addition, we have

$$\boldsymbol{B}^{+T}\boldsymbol{\omega} = (\boldsymbol{\omega}^T\boldsymbol{b}^T, \boldsymbol{\omega}^T\boldsymbol{P}\boldsymbol{b}^T, \boldsymbol{\omega}^T\boldsymbol{P}^2\boldsymbol{b}^T, \cdots, \boldsymbol{\omega}^T\boldsymbol{P}^{n-1}\boldsymbol{b}^T)^T. \tag{26}$$

Note that the summation of the phase difference between two neighboring oscillators along the ring structure is zero. We consider a special case that n is an even number and $\omega_i = -\omega_{i+n/2}$, which is equivalent to that $\boldsymbol{P}^{n/2}\boldsymbol{\omega} = -\boldsymbol{\omega}$. This means that summation of all terms of $\arcsin\frac{\boldsymbol{B}^{+T}\boldsymbol{\omega}}{\lambda}$ is zero. Therefore, a necessary condition for synchronization is

$$\lambda_c = \|\boldsymbol{B}^{+T}\boldsymbol{\omega}\|_\infty = \max_\alpha|[\boldsymbol{B}^{+T}\boldsymbol{\omega}]_\alpha|, \tag{27}$$

where the maximum function runs over all links α. ♯

Remark 4. Suppose $\omega_i = \sin\frac{2\pi i}{n}$ and $n = 10$, we have $\lambda_c = \sin\frac{\pi}{5} + \sin\frac{2\pi}{5} \approx 1.539$.

4. Product of synchronization transitions

In the following, we first summarize the results of the synchronization transitions of the Kuramoto model on a single network (star and ring).

(i) For n oscillators coupled in a star structure.
We consider the special case of explosive transitions to synchronization [13, 36]. In particular, we assume that the hub node has the frequency $\omega_1 = (n-1)\omega$ and all leaf nodes have the same frequency $\omega_2 = \omega_3 = \cdots = \omega_n = \omega$. A necessary condition for synchronization yields the critical coupling

Table 1. Hysteresis area $\Delta\lambda$ on $G_1\square G_2$ if both factors G_1 and G_2 are stars.

Regime	$\lambda_{c1}^f > \lambda_{c2}^f$	$\lambda_{c1}^f < \lambda_{c2}^f$
$\lambda_{c1}^b > \lambda_{c2}^b$	$\lambda_{c1}^f - \lambda_{c1}^b$	$\lambda_{c2}^f - \lambda_{c1}^b$
$\lambda_{c1}^f < \lambda_{c2}^f$	$\lambda_{c1}^f - \lambda_{c2}^f$	$\lambda_{c2}^f - \lambda_{c2}^f$

Table 2. Synchronization types on $G_1\square G_2$ if factor G_1 is a star and G_2 is a ring.

Case	$\lambda_{c2} < \lambda_{c1}^b$	$\lambda_{c1}^b \leqslant \lambda_{c2} < \lambda_{c1}^f$	$\lambda_{c2} \geqslant \lambda_{c1}^f$
Thresholds	λ_{c1}^f, λ_{c1}^b of G_1	λ_{c1}^f of G_1 and λ_{c2} of G_2	λ_{c2} of G_2
Sync type	Only discontinuous transitions	Discontinuous transition for the forward curve and continuous transition for the backward curve	Only continuous transitions

threshold $\lambda_c^b = \frac{n-2}{n}\omega$ [13, 36]. Starting from an incoherent state and increasing the coupling strength, the network experiences a transition to synchronization at the critical coupling $\lambda_c^f = \frac{n-2}{\sqrt{2n-1}}$ [36]. Both synchronization transitions are discontinuous and the crucial property of the two transition thresholds is that $\lambda_c^f > \lambda_c^b$, which leads to a clear hysteretic area $\Delta\lambda = \lambda_c^f - \lambda_c^b$. We refer the readers to the [13, 36] for the detailed derivations of the critical coupling λ_c^f for the forward transition to synchronization.

(ii) For n oscillators coupled on a ring structure.
According to corollary 2, we consider the special case that there is an even number of n oscillators and frequency is $\omega_i = -\omega_{i+n/2}$. The system presents a continuous synchronization transition at λ_c. No hysteresis exists since both the backward and forward transition curves are overlapped.

In this work, we focus on the dynamics of the Kuramoto model when performing the Cartesian product from two factor graphs. It is certainly an interesting topic to discuss the structural properties of the resulting product graph, which however is outside the scope of the present work. Given two independent networks of phase oscillators on G_1 and G_2 (e.g., G_1 is a star and G_2 is a ring), the synchronization transitions on the Cartesian product $G_1\square G_2$ graph are summarized in the following:

(i) A discontinuous synchronization transition is obtained if both G_1 and G_2 are star networks.
Suppose that λ_{c1}^b, λ_{c1}^f are two threshold values for G_1 and, furthermore, $\lambda_{c1}^f > \lambda_{c1}^b$, which yields the hysteretic size $\Delta\lambda_{c1} = \lambda_{c1}^f - \lambda_{c1}^b$. In a full analogy, thresholds for G_2 are assumed to be $\lambda_{c2}^f > \lambda_{c2}^b$ and $\Delta\lambda_{c2} = \lambda_{c2}^f - \lambda_{c2}^b$. On the Cartesian product $G_1\square G_2$, we obtain discontinuous synchronization transition and the hysteretic area $\Delta\lambda$ is summarized in table 1.

(ii) A continuous synchronization transition is obtained if both G_1 and G_2 are ring networks.
Suppose that λ_{c1} is the critical coupling threshold value for G_1, and respectively, λ_{c2} is for G_2. The critical coupling on the product graph $G_1\square G_2$ is $\lambda_c = \max\{\lambda_{c1}, \lambda_{c2}\}$.

(iii) A mixture of continuous and discontinuous synchronization transition is obtained if G_1 is a star and G_2 is a ring network.
Again, we suppose that λ_{c1}^b, λ_{c1}^f are two thresholds for G_1 and the hysteresis size is $\Delta\lambda = \lambda_{c1}^f - \lambda_{c1}^b$. For G_2, the threshold is λ_{c2}. On the product $G_1\square G_2$, the synchronization transitions are summarized in table 2. If λ_{c2} is smaller than λ_{c1}^b, both the forward and backward curves collide with the synchronization transitions on G_1. Namely, only discontinuous transitions are observed for $G_1\square G_2$.
If $\lambda_{c1}^b \leqslant \lambda_{c2} < \lambda_{c1}^f$, the forward transition is discontinuous at λ_{c1}^f and the backward transition is continuous at λ_{c2}. If $\lambda_{c2} \geqslant \lambda_{c1}^f$, only continuous transitions are possible at λ_{c2}. For the numerical studies below, we consider the case of $\lambda_{c1}^b \leqslant \lambda_{c2} < \lambda_{c1}^f$ when we observe a mixture state of synchronization transitions.

For a numerical simulation purpose, we choose equal sizes $n_1 = n_2 = 10$ for the factors G_1 and G_2. In the case of star networks, the natural frequency is chosen as $\boldsymbol{\omega}^{(1)} = (9,1,\cdots,1)^T$ for G_1 and $\boldsymbol{\omega}^{(2)} = 0.6\boldsymbol{\omega}^{(1)}$ for G_2. In the case of rings, the frequency is chosen as $\omega_i^{(1)} = \sin(2\pi \mathrm{i}/n_1)$ for G_1 and $\omega_i^{(2)} = 0.6\sin(2\pi \mathrm{i}/n_2)$ for G_2. The choice of natural frequencies yields different critical coupling thresholds for G_1 and G_2, which are listed in table 3 and are further illustrated in figure 2. In particular, we observe discontinuous transitions in both forward and backward directions if the product graph $G_1\square G_2$ is obtained from two star networks, where we find a clear hysteresis as shown in figures 2(a)–(d). If the product $G_1\square G_2$ is reconstructed from two ring networks, only

Table 3. Critical coupling thresholds on $G_1 \square G_2$ as shown in figure 2.

	Star	Ring	One star and one ring
G_1	$\lambda_{c1}^b = 0.8,\ \lambda_{c1}^f = 1.84$	$\lambda_{c1} = 1.54$	$\lambda_{c1}^b = 0.80,\ \lambda_{c1}^f = 1.84$
G_2	$\lambda_{c2}^b = 0.48,\ \lambda_{c2}^f = 1.10$	$\lambda_{c2} = 0.92$	$\lambda_{c2} = 0.92$
$G_1 \square G_2$	$\lambda_c^b = 0.80,\ \lambda_c^f = 1.84$	$\lambda_c = 1.54$	$\lambda_c^b = 0.92,\ \lambda_c^f = 1.84$
Hysteresis	Yes	No	Yes

continuous transitions are observed in figures 2(e)–(h). In addition, if G_1 is a star and G_2 is a ring, the product graph $G_1 \square G_2$ presents a mixture state of continuous transition for the backward direction and a discontinuous one for the forward direction, showing hysteretic behavior as shown in figures 2(i)–(l). In all these cases, the theoretical predictions for synchronization transitions are perfectly validated by our numerical simulations, which are highlighted by vertical dashed lines.

5. Discussion

In summary, we have provided theoretical analysis on effects of graph operations on synchronization transitions in the Kuramoto models, in particular with the Cartesian product. Given two independent Kuramoto models on different topologies, where the individual systems present either continuous or discontinuous transitions to synchronization. Taking into account different network topologies (star, chain, ring, and tree), we proposed a unified framework in obtaining necessary conditions for synchronization in each network structure, which is based on a detailed analysis of the existence of solutions to linear equations (18). Under the phase summation assumption, the results as summarized in the theorem and lemma can be easily generalized to the case of n factor subgraphs because of the commutative and associative properties of the Cartesian product operation.

Rich synchronization transitions have been obtained for the Cartesian product graph. Depending on the relation between the critical coupling thresholds, there are three different synchronization scenarios on the Cartesian product graph: (i) both the forward and backward transitions are discontinuous with a clear hysteresis area, (ii) both the forward and backward transitions are continuous and these two curves are overlapped and, hence, without hysteresis, and (iii) the forward transition from an incoherent state to a coherent one is discontinuous and the backward transition from a coherent state to an incoherent one is continuous with a hysteretic behavior.

In this work, our theoretical approaches are mainly focused on star, chain and ring structures because the necessary conditions of synchronization transitions have been analytically obtained in the same framework. From the viewpoint of numerical simulations, the phase summation operation on the Cartesian product graph can be performed for general network settings as well. For instance, given two independent factors G_1 and G_2 presenting continuous synchronization transitions at respective critical couplings λ_{c1} and λ_{c2}, the synchronization on the product graph $G_1 \square G_2$ is fully determined by the product $R = R_1 R_2$. Therefore, the critical coupling on $G_1 \square G_2$ is $\lambda_c = \max\{\lambda_{c1}, \lambda_{c2}\}$.

The Cartesian product can be performed recursively, for instance, by Kronecker power, which is one of the graph operations in generating a big graph from two or more small factor graphs [37]. This generative model presents some properties that are often observed in real networks, e.g., in heavy-tailed degree distributions and small diameters etc. From the viewpoint of illustration, it shares some similarities with generating multi-layer networks [8]. Therefore, our results provide some novel insight in network design and synchronization control.

Acknowledgments

This work is in part financially supported by Natural Science Foundation of Shanghai (Grant No. 17ZR1444800).

Appendix A. Kronecker product and Kronecker sum

Definition (Kronecker product of matrices). Given two matrices $\boldsymbol{A}^{(1)} = [a_{ij}^{(1)}]$ and $\boldsymbol{A}^{(2)} = [a_{ij}^{(2)}]$ of sizes $m \times n$ and $r \times s$ respectively, the Kronecker product matrix $\boldsymbol{A}^{(1)} \otimes \boldsymbol{A}^{(2)}$ of dimensions $mr \times ns$ is given by

$$\boldsymbol{A}^{(1)} \otimes \boldsymbol{A}^{(2)} = \begin{pmatrix} a_{11}^{(1)}\boldsymbol{A}^{(2)} & a_{12}^{(1)}\boldsymbol{A}^{(2)} & \dots & a_{1n}^{(1)}\boldsymbol{A}^{(2)} \\ a_{21}^{(1)}\boldsymbol{A}^{(2)} & a_{22}^{(1)}\boldsymbol{A}^{(2)} & \dots & a_{2n}^{(1)}\boldsymbol{A}^{(2)} \\ \vdots & \vdots & \ddots & \vdots \\ a_{m1}^{(1)}\boldsymbol{A}^{(2)} & a_{m2}^{(1)}\boldsymbol{A}^{(2)} & \dots & a_{mn}^{(1)}\boldsymbol{A}^{(2)} \end{pmatrix}. \tag{A.1}$$

Each element of the product matrix is hence represented by $A_{ij}^{(1)}A_{kl}^{(2)}$.

Definition (Kronecker sum of matrices). Suppose two matrices $\boldsymbol{A}^{(1)}$ and $\boldsymbol{A}^{(2)}$ of sizes $m \times m$ and $n \times n$ respectively, the Kronecker sum matrix $\boldsymbol{A}^{(1)} \oplus \boldsymbol{A}^{(2)}$ has dimensions $mn \times mn$, which is given by

$$\boldsymbol{A}^{(1)} \oplus \boldsymbol{A}^{(2)} = \boldsymbol{A}^{(1)} \otimes \boldsymbol{I}_n + \boldsymbol{I}_m \otimes \boldsymbol{A}^{(2)}, \tag{A.2}$$

where $\boldsymbol{I}_m$, $\boldsymbol{I}_n$ are identity matrices of dimension $m \times m$ and $n \times n$ respectively. Each element of the sum matrix is hence represented by $A_{ij}^{(1)}\delta_{kl} + \delta_{ij}A_{kl}^{(2)}$, where δ_{ij} are Kronecker delta functions.

Appendix B. Equivalence between equations (15) and (1)

Proof. We show the coupling terms of both representations are identical. Suppose two phase oscillators attached to the link α are denoted as α^+ and α^-, where α^+ is the starting point while α^- is the end point respectively. Thus we have the notation $[\boldsymbol{B\theta}]_\alpha = \theta_{\alpha^+} - \theta_{\alpha^-}$. Therefore, the coupling term for the node i is expanded as

$$[\boldsymbol{B}^T \sin \boldsymbol{B\theta}]_i = \sum_{\alpha=1}^{m} B_{\alpha i} \sin(\theta_{\alpha^+} - \theta_{\alpha^-}). \tag{B.1}$$

If oscillator i is the starting point $i = \alpha^+$, and j is the end point $j = \alpha^-$

$$B_{\alpha i} \sin(\theta_{\alpha^+} - \theta_{\alpha^-}) = \sin(\theta_i - \theta_j). \tag{B.2}$$

On the other hand, if i is the end point $i = \alpha^-$, and j is the starting point $j = \alpha^-$, we have

$$B_{\alpha i} \sin(\theta_{\alpha^+} - \theta_{\alpha^-}) = -\sin(\theta_j - \theta_i) = \sin(\theta_i - \theta_j). \tag{B.3}$$

Therefore the coupling term of node i is simplified as

$$\sum_{\alpha=1}^{m} B_{\alpha i} \sin(\theta_{\alpha^+} - \theta_{\alpha^-}) = \sum_{j=1}^{n} A_{ij} \sin(\theta_i - \theta_j). \tag{B.4}$$

This proves the statement that the coupling terms are identical in equations (15) and (1). ♯

Appendix C. Moore–Penrose pseudo-inverse

Here we give a brief introduction to the Moore–Penrose pseudo-inverse, a generalization of the inverse of a matrix. The Moore–Penrose pseudo-inverse is defined for any matrix and is unique, which brings conceptual clarity to study the solutions of arbitrary systems of linear equations.

Definitions. Suppose $\boldsymbol{A} \in \mathbb{R}^{m\times n}$. Then $\{\boldsymbol{Ax}|\boldsymbol{x} \in \mathbb{R}^n\}$ is a linear subspace of $\mathbb{R}^m$, which is called the image space of $\boldsymbol{A}$ and denoted as Im $\boldsymbol{A}$. $\{\boldsymbol{x} \in \mathbb{R}^n|\boldsymbol{Ax} = \boldsymbol{0}\}$ is a linear subspace of $\mathbb{R}^n$, which is called the kernel of A and denoted as ker $\boldsymbol{A}$. In addition, due to the Fredholm theory, we have $(\text{Im } \boldsymbol{A})^\perp = \ker \boldsymbol{A}^T$ and $(\ker \boldsymbol{A})^\perp = \text{Im } \boldsymbol{A}^T$, where $\perp$ is the orthogonal complement space.

For $\boldsymbol{A} \in \mathbb{R}^{m\times n}$, there exists a unique matrix $\boldsymbol{X} \in \mathbb{R}^{n\times m}$ which is called the Moore–Penrose pseudo-inverse of $\boldsymbol{A}$ if and only if the following four criteria are satisfied: (i) $\boldsymbol{AXA} = \boldsymbol{A}$, (ii) $\boldsymbol{XAX} = \boldsymbol{X}$, (iii) $(\boldsymbol{AX})^T = \boldsymbol{AX}$, (iv) $(\boldsymbol{XA})^T = \boldsymbol{XA}$. We denote the Moore–Penrose pseudo-inverse of $\boldsymbol{A}$ as $\boldsymbol{A}^+$. Note that $\boldsymbol{A}^+$ exists for any matrix $\boldsymbol{A}$ and furthermore $\boldsymbol{A}^+$ is equivalent to the inverse $\boldsymbol{A}^{-1}$ if $\boldsymbol{A}$ has full rank. In addition, we denote the transpose of $\boldsymbol{A}^+$ as $\boldsymbol{A}^{+T}$ and we have $(\boldsymbol{A}^T)^+ = (\boldsymbol{A}^+)^T$. Additional property of pseudo-inverse is $\ker \boldsymbol{A}^+ = \ker \boldsymbol{A}^T$.

The Moore–Penrose pseudo-inverse theorem is effectively for studying the solution of arbitrary systems of linear equations. For a linear system $\boldsymbol{Ax} = \boldsymbol{b}$, $\boldsymbol{A} \in \mathbb{R}^{m\times n}$ and $\boldsymbol{b} \in \mathbb{R}^m$. (i) No solution exists if $\text{rank}\boldsymbol{A} < \text{rank}(\boldsymbol{A}, \boldsymbol{b})$; (ii) unique solution exists if $\text{rank}\boldsymbol{A} = \text{rank}(\boldsymbol{A}, \boldsymbol{b}) = n$ and the solution reads $\boldsymbol{x} = \boldsymbol{A}^+\boldsymbol{b}$; (iii) infinite number of solutions exist if $\text{rank}\boldsymbol{A} = \text{rank}(\boldsymbol{A}, \boldsymbol{b}) < n$ and the solutions read $\boldsymbol{x} = \boldsymbol{A}^+\boldsymbol{b} + (\boldsymbol{I} - \boldsymbol{A}^+\boldsymbol{A})\boldsymbol{u}$ where $\boldsymbol{u} \in \mathbb{R}^n$ is an arbitrary vector, and $(\boldsymbol{I} - \boldsymbol{A}^+\boldsymbol{A})\boldsymbol{u} \in \ker \boldsymbol{A}$.

Appendix D. Solutions to linear equations (18)

We first consider a general solution $\boldsymbol{x}$ to the system

$$\boldsymbol{B}^T\boldsymbol{x} = \boldsymbol{\omega} - \bar{\boldsymbol{\omega}}, \tag{D.1}$$

where $\boldsymbol{x} = \lambda \sin \boldsymbol{B\theta}$. A solution always exists if the condition $\boldsymbol{\omega} - \bar{\boldsymbol{\omega}} \in \mathrm{Im}\ \boldsymbol{B}^T$ holds, or equivalently if the condition $\boldsymbol{\omega} - \bar{\boldsymbol{\omega}} \perp \ker \boldsymbol{B}$ holds (Fredholm expression).

Corollary 3. *A solution always exists for connected networks.*

Proof. For a connected network, we have $\ker \boldsymbol{B} = \mathrm{span}\{\mathbf{1}\}$ and

$$\mathbf{1}^T(\boldsymbol{\omega} - \bar{\boldsymbol{\omega}}) = \sum_{i=1}^{n} \omega_i - \sum_{i=1}^{n} \bar{\omega} = 0. \tag{D.2}$$

Therefore, the condition $\boldsymbol{\omega} - \bar{\boldsymbol{\omega}} \perp \ker \boldsymbol{B}$ holds. ♯

In the following, we consider two cases:

Case 1. $\mathrm{rank}\boldsymbol{B}^T = n - 1 = m$, which holds for any tree topology without any loops. Because $\ker \boldsymbol{B}^{+T} = \ker \boldsymbol{B}$ and $\boldsymbol{B}^{+T}\bar{\boldsymbol{\omega}} = 0$, a unique solution reads

$$\boldsymbol{x} = \boldsymbol{B}^{+T}\boldsymbol{\omega}. \tag{D.3}$$

Since the incidence matrix $\boldsymbol{B}$ is row full rank, the general solution in terms of $\boldsymbol{\theta}$ to the linear system reads

$$\boldsymbol{\theta} = \boldsymbol{B}^{+}\arcsin\frac{\boldsymbol{B}^{+T}\boldsymbol{\omega}}{\lambda} + (\boldsymbol{I}_n - \boldsymbol{B}^{+}\boldsymbol{B})\boldsymbol{\nu}, \tag{D.4}$$

where $(\boldsymbol{I}_n - \boldsymbol{B}^{+}\boldsymbol{B})\boldsymbol{\nu} \in \ker \boldsymbol{B} = \mathrm{span}\ \{\mathbf{1}\}$, and $\boldsymbol{\nu}$ is an arbitrary vector. Note that the arbitrary vector $\boldsymbol{\nu}$ adds a constant to each phase component, which is equivalent to use a rotating frame with this constant to the ensemble of oscillators. Neglecting the term of arbitrary vector $\boldsymbol{\nu}$, the synchronized solution reads

$$\boldsymbol{\theta} = \boldsymbol{B}^{+}\arcsin\frac{\boldsymbol{B}^{+T}\boldsymbol{\omega}}{\lambda}. \tag{D.5}$$

Since the sine functions are bounded, the existence condition for synchronization is

$$\lambda \geqslant \lambda_c = \|\boldsymbol{B}^T\boldsymbol{\omega}\|_\infty = \max_\alpha |[\boldsymbol{B}^T\boldsymbol{\omega}]_\alpha|, \tag{D.6}$$

where the maximum norm runs over all links α.

Case 2. $\mathrm{rank}\boldsymbol{B}^T = n - 1 < m$, which is typical for a general complex network topology with loop structures. Considering $\boldsymbol{B}^{+T}\bar{\boldsymbol{\omega}} = 0$, an infinite number of solutions reads

$$\boldsymbol{x} = \boldsymbol{B}^{+T}\boldsymbol{\omega} + (\boldsymbol{I}_m - \boldsymbol{B}^{+T}\boldsymbol{B}^T)\boldsymbol{u}. \tag{D.7}$$

where $\boldsymbol{u}$ is an arbitrary vector. In terms of $\boldsymbol{\theta}$, the solution reads

$$\boldsymbol{B\theta} = \arcsin\frac{\boldsymbol{B}^{+T}\boldsymbol{\omega} + (\boldsymbol{I}_m - \boldsymbol{B}^{+T}\boldsymbol{B}^T)\boldsymbol{u}}{\lambda}. \tag{D.8}$$

Solutions of $\boldsymbol{\theta}$ do not always exist because $\boldsymbol{B}$ is not row full rank. In addition, the summation of phase difference between two neighboring oscillators along the loop structure is zero, which suggests that the choice of $\boldsymbol{u}$ can not be arbitrary.

If synchronization exists ($\lambda \geqslant \lambda_c$), a general solution of $\boldsymbol{\theta}$ reads

$$\boldsymbol{\theta} = \boldsymbol{B}^{+}\arcsin\frac{\boldsymbol{B}^{+T}\boldsymbol{\omega} + (\boldsymbol{I}_m - \boldsymbol{B}^{+T}\boldsymbol{B}^T)\boldsymbol{u}}{\lambda} + (\boldsymbol{I}_n - \boldsymbol{B}^{+}\boldsymbol{B})\boldsymbol{\nu}. \tag{D.9}$$

Note that, as in the case (i), the arbitrary vector $\boldsymbol{\nu}$ adds a constant to each phase component, which is equivalent to use a rotating frame with this constant to the ensemble of oscillators. Neglecting the term of arbitrary vector $\boldsymbol{\nu}$, the synchronized solution reads

$$\boldsymbol{\theta} = \boldsymbol{B}^{+}\arcsin\frac{\boldsymbol{B}^{+T}\boldsymbol{\omega} + (\boldsymbol{I}_m - \boldsymbol{B}^{+T}\boldsymbol{B}^{T})\boldsymbol{u}}{\lambda}. \tag{D.10}$$

Because sine functions are bounded, the existence of synchronization solutions yields the necessary condition as

$$\lambda \geqslant \lambda_c = \|\boldsymbol{B}^{+T}\boldsymbol{\omega} + (\boldsymbol{I}_m - \boldsymbol{B}^{+T}\boldsymbol{B}^{T})\boldsymbol{u}\|_{\infty}, \tag{D.11}$$

where $\|\cdot\|$ is the maximum norm.

Appendix E. Kuramoto model on a chain

Corollary 4. *For n oscillators coupled in a chain, the necessary condition of synchronization is* $\lambda \geqslant \lambda_c = \max_{1\leqslant k\leqslant n-1}|\sum_{i=1}^{k}(\omega_i - \bar{\omega})|$.

Proof. The incidence matrix

$$\boldsymbol{B} = \begin{pmatrix} 1 & -1 & 0 & \dots & 0 & 0 \\ 0 & 1 & -1 & \dots & 0 & 0 \\ \vdots & \vdots & \vdots & \ddots & \vdots & \vdots \\ 0 & 0 & 0 & \dots & 1 & -1 \end{pmatrix} \tag{E.1}$$

and the Moore–Penrose pseudo-inverse reads

$$\boldsymbol{B}^{+T} = \begin{pmatrix} \frac{n-1}{n} & -\frac{1}{n} & -\frac{1}{n} & \cdots & -\frac{1}{n} \\ \frac{n-2}{n} & -\frac{n-2}{n} & -\frac{2}{n} & \cdots & -\frac{2}{n} \\ \vdots & \vdots & \vdots & \ddots & \vdots \\ \frac{1}{n} & \frac{1}{n} & \frac{1}{n} & \cdots & -\frac{n-1}{n} \end{pmatrix}. \tag{E.2}$$

In addition, we have

$$\boldsymbol{B}^{+T}\boldsymbol{\omega} = \begin{pmatrix} \omega_1 - \bar{\omega} \\ \omega_1 + \omega_2 - 2\bar{\omega} \\ \vdots \\ \bar{\omega} - \omega_n \end{pmatrix}. \tag{E.3}$$

Hence the necessary condition of synchronization is

$$\lambda_c = \max_{1\leqslant k\leqslant n-1}\left|\sum_{i=1}^{k}\omega_i - \bar{\omega}\right|. \sharp \tag{E.4}$$

Remark 5. For a special case of three oscillators coupled in a chain, we have the critical coupling strength for synchronization as $\lambda_c = \max\{|\omega_1 - \bar{\omega}|, |\omega_3 - \bar{\omega}|\}$ where $\bar{\omega} = (\omega_1 + \omega_2 + \omega_3)/3$, which is the same as the case of corollary 1.

Appendix F. Kuramoto model on a tree—a universal model for star and chain structures

A tree structure becomes two disjoint components A and B when any link α is removed. We denote the two oscillators attached to the link α by a in the component A and, respectively, b in the component B. With the notations of the average phase of all oscillators $\bar{\theta}$ and the average frequency $\bar{\omega}$ (equation (16)), the compact form of synchronization (equation (17)) in the components A and B are expressed as

$$\sum_{i\in A}\left(\frac{\mathrm{d}\theta_i}{\mathrm{d}t} - \frac{\mathrm{d}\bar{\theta}}{\mathrm{d}t}\right) = \sum_{i\in A}(\omega_i - \bar{\omega}) + \lambda\sin(\theta_b - \theta_a), \tag{F.1}$$

$$\sum_{i\in B}\left(\frac{\mathrm{d}\theta_i}{\mathrm{d}t} - \frac{\mathrm{d}\bar{\theta}}{\mathrm{d}t}\right) = \sum_{i\in B}(\omega_i - \bar{\omega}) + \lambda\sin(\theta_a - \theta_b). \tag{F.2}$$

It is sufficient to consider equation (F.1) only since the sum of the above two equations ((F.1) and (F.2)) is zero. Furthermore, synchronization is achieved when the phase difference between each oscillator and the average phase is a constant, namely, we have $\frac{\mathrm{d}\theta_i}{\mathrm{d}t} - \frac{\mathrm{d}\bar{\theta}}{\mathrm{d}t} = 0$. Therefore, the equation (F.1) in the component A is rewritten as

$$\sum_{i\in A}(\omega_i - \bar{\omega}) + \lambda\sin(\theta_b - \theta_a) = 0, \tag{F.3}$$

which is further simplified as

$$\sum_{i\in A}(\omega_i - \bar{\omega}) = -\lambda \sin(\theta_b - \theta_a). \tag{F.4}$$

Because the sine function is bounded, the synchronization solution exists if the following condition

$$\lambda \geqslant \lambda_\alpha = \left| \sum_{i\in A}(\omega_i - \bar{\omega}) \right| \tag{F.5}$$

is fulfilled. Performing the same analysis for each link α in the component A, we obtain the necessary condition for synchronization as

$$\lambda \geqslant \max_{1\leqslant\alpha\leqslant m} \lambda_\alpha = \max_{1\leqslant\alpha\leqslant m} \left| \sum_{i\in A_\alpha} (\omega_i - \bar{\omega}) \right| . \tag{F.6}$$

Note that the equation (F.6) has the explicit form of equation (22) for a star and equation (E.4) for a chain, respectively.

ORCID iDs

Yong Zou https://orcid.org/0000-0002-3241-3139

References

[1] Pikovsky A, Rosenblum M and Kurths J 2001 *Synchronization—A Universal Concept in Nonlinear Sciences* (Cambridge : Cambridge University Press)
[2] Strogatz S H 2000 From Kuramoto to Crawford: exploring the onset of synchronization in populations of coupled oscillators *Physica* D **143** 1–20
[3] Acebrón J A, Bonilla L L, Pérez Vicente C J, Ritort F and Spigler R 2005 The Kuramoto model: a simple paradigm for synchronization phenomena *Rev. Mod. Phys.* **77** 137–85
[4] Kuramoto Y 1975 Self-entrainment of a population of coupled nonlinear oscillators *International Symposium on Mathematical Problems in Theoretical Physics* (Berlin: Springer) pp 420–2
[5] Kuramoto Y 1984 *Chemical Oscillations, Waves, and Turbulence* (Berlin: Springer)
[6] Moreno Y and Pacheco A F 2004 Synchronization of Kuramoto oscillators in scale-free networks *Europhys. Lett.* **68** 603–9
[7] Arenas A, Diaz-Guilera A, Kurths J, Moreno Y and Zhou C S 2008 Synchronization in complex networks *Phys. Rep.* **469** 93–153
[8] Boccaletti S, Bianconi G, Criado R, del Genio C I, Gómez-Gardeñes J, Romance M, Sendiña-Nadal I, Wang Z and Zanin M 2014 The structure and dynamics of multilayer networks *Phys. Rep.* **544** 1–122
[9] Rodrigues F A, Peron T K D M, Ji P and Kurths J 2016 The Kuramoto model in complex networks *Phys. Rep.* **610** 1–98
[10] Gómez-Gardeñes J, Moreno Y and Arenas A 2007 Paths to synchronization on complex networks *Phys. Rev. Lett.* **98** 034101
[11] Gómez-Gardeñes J, Gómez S, Arenas A and Moreno Y 2011 Explosive synchronization transitions in scale-free networks *Phys. Rev. Lett.* **106** 128701
[12] Leyva I, Sevilla-Escoboza R, Buldú J M, Sendiña Nadal I, Gómez-Gardeñes J, Arenas A, Moreno Y, Gómez S, Jaimes-Reátegui R and Boccaletti S 2012 Explosive first-order transition to synchrony in networked chaotic oscillators *Phys. Rev. Lett.* **108** 168702
[13] Zou Y, Pereira T, Small M, Liu Z H and Kurths J 2014 Basin of attraction determines hysteresis in explosive synchronization *Phys. Rev. Lett.* **112** 114102
[14] Zhang X Y, Boccaletti S, Guan S G and Liu Z H 2015 Explosive synchronization in adaptive and multilayer networks *Phys. Rev. Lett.* **114** 038701
[15] Boccaletti S, Almendral J A, Guan S, Leyva I, Liu Z, Sendiña-Nadal I, Wang Z and Zou Y 2016 Explosive transitions in complex networks' structure and dynamics: percolation and synchronization *Phys. Rep.* **660** 1–94
[16] Peron T K D and Rodrigues F A 2012 Determination of the critical coupling of explosive synchronization transitions in scale-free networks by mean-field approximations *Phys. Rev.* E **86** 056108
[17] Leyva I, Navas A, Sendiña Nadal I, Almendral J A, Buldú J M, Zanin M, Papo D and Boccaletti S 2013 Explosive transitions to synchronization in networks of phase oscillators *Sci. Rep.* **3** 1281–5
[18] Peron T K D and Rodrigues F A 2012 Explosive synchronization enhanced by time-delayed coupling *Phys. Rev.* E **86** 016102
[19] Ji P, Peron T K D M, Menck P J, Rodrigues F A and Kurths J 2013 Cluster explosive synchronization in complex networks *Phys. Rev. Lett.* **110** 218701
[20] Zhang Y Z, Nishikawa T and Motter A E 2017 Asymmetry-induced synchronization in oscillator networks *Phys. Rev.* E **95** 062215
[21] Skardal P S and Arenas A 2014 Disorder induces explosive synchronization *Phys. Rev.* E **89** 062811
[22] Zhang X Y, Hu X, Kurths J and Liu Z H 2013 Explosive synchronization in a general complex network *Phys. Rev.* E **88** 010802
[23] Bi H J, Hu X, Boccaletti S, Wang X G, Zou Y, Liu Z H and Guan S G 2016 Coexistence of quantized, time dependent, clusters in globally coupled oscillators *Phys. Rev. Lett.* **117** 204101
[24] Hammack R, Imrich W and Klavzar S 2011 *Handbook of Product Graphs: Structure and Recognition* 2nd edn (London: Taylor and Francis)
[25] Atay F M and Bıyıkoğlu T 2005 Graph operations and synchronization of complex networks *Phys. Rev.* E **72** 016217
[26] Duan Z S, Liu C and Chen G R 2008 Network synchronizability analysis: the theory of subgraphs and complementary graphs *Physica* D **237** 1006–12
[27] Imrich W, Klavzar S and Rall D F 2008 *Topics in Graph Theory: Graphs and Their Cartesian Product* (Boca Raton, FL: A K Peters/CRC Press)
[28] Strogatz S H 2001 Exploring complex networks *Nature* **410** 268–76
[29] Ermentrout G B and Kopell N 1984 Frequency plateaus in a chain of weakly coupled oscillators, I *SIAM J. Math. Anal.* **15** 215–37

[30] Emelianova Y P, Kuznetsov A P, Sataev I R and Turukina L V 2013 Synchronization and multi-frequency oscillations in the low-dimensional chain of the self-oscillators *Physica* D **244** 36–49
[31] Díaz-Guilera A and Arenas A 2008 Phase patterns of coupled oscillators with application to wireless communication *Bio-Inspired Computing and Communication: First Workshop on Bio-Inspired Design of Networks, BIOWIRE 2007 (Cambridge, UK, 2–5, April, 2007)* ed P Liò *et al* (Berlin: Springer) pp 184–91 Revised Selected Papers
[32] Ottino-Löffler B and Strogatz S H 2016 Comparing the locking threshold for rings and chains of oscillators *Phys. Rev.* E **94** 062203
[33] Pereira T 2010 Hub synchronization in scale-free networks *Phys. Rev.* E **82** 036201
[34] Ha S Y and Kang M J 2012 On the basin of attractors for the unidirectionally coupled Kuramoto model in a ring *SIAM J. Appl. Math.* **72** 1549–74
[35] Bergner A, Frasca M, Sciuto G, Buscarino A, Ngamga E J, Fortuna L and Kurths J 2012 Remote synchronization in star networks *Phys. Rev.* E **85** 026208
[36] Vlasov V, Zou Y and Pereira T 2015 Explosive synchronization is discontinuous *Phys. Rev.* E **92** 012904
[37] Leskovec J, Chakrabarti D, Kleinberg J, Faloutsos C and Ghahramani Z 2010 Kronecker graphs: an approach to modeling networks *J. Mach. Learn. Res.* **11** 985–1042